Optical properties of the charge-density-wave compound $CeTe_2$

K. E. Lee,[1] C. I. Lee,[1] H. J. Oh,[1,2] M. A. Jung,[1] B. H. Min,[1] H. J. Im,[1] T. Iizuka,[3] Y. S. Lee,[4] S. Kimura,[3] and Y. S. Kwon[1,*]

[1]*Department of Physics, Sungkyunkwan University, Suwon 440-746, Republic of Korea*

[2]*Department of Ophthalmic Optics, Masan College, Masan 630-729, Republic of Korea*

[3]*UVSOR Facility, Institute for Molecular Science, Okazaki 444-8585, Japan*

[4]*Department of Physics, Soongsil University, Seoul 156-734, Republic of Korea*

(Received 22 May 2008; revised manuscript received 9 September 2008; published 10 October 2008)

The temperature dependence of the optical conductivity of $CeTe_2$ was obtained for the $E\|ab$ plane and $E\|c$ axis at photon energies ranging from terahertz to visible light. Two gap states are found in the optical conductivity spectra. The magnitudes of the gaps are estimated to be 0.448 and 0.109 eV in the $E\|ab$ plane. The former is due to perfect nesting, while the latter is due to imperfect nesting. The magnitude of the gap due to perfect nesting on the c axis is evaluated to be 0.854 eV. The Drude response caused by the ungapped Fermi surface is found only on the $E\|ab$ plane since $CeTe_2$ is a quasi-two-dimensional material. The portion of the ungapped Fermi surface across all Fermi surfaces is about 3%.

DOI: 10.1103/PhysRevB.78.134408 PACS number(s): 71.45.Lr, 78.20.−e, 71.20.Eh

I. INTRODUCTION

$CeTe_2$ has attracted attention due to its effective low dimensionality. It plays host to a charge-density wave (CDW) and can be described in terms of a modulated Cu_2Sb-type structure (Pa/nmm) based on alternating layers of square-planar Te sheets and a corrugated CeTe slab.[1–3] Band-structure calculations for the stoichiometric material indicate a strongly anisotropic Fermi surface (FS) with a predominately Te $5p$ character having minimal c-axis dispersion, a large region of which is nested.[3–5] A substantial anisotropy in the electrical resistivity along different crystallographic directions confirms the quasi-two-dimensional (2D) character of the charge carriers. The resistivity ratio (ρ_c/ρ_{ab}) between the c axis and the ab plane at $T=0.7$ K is about 125.[6] The temperature dependence of the electrical resistivity is reminiscent of either a semimetal or a doped small-gap semiconductor and differs significantly from that of a good metal.

A superlattice modulation of the average structure has been observed at room temperature via transmission electron microscopy (TEM) (Ref. 3) and x-ray diffraction.[7] These observations show that the lattice modulation was a CDW driven by electronic instability of the Fermi surface. Tunneling measurements[1] and infrared spectroscopy[8] have clearly revealed a well-developed CDW gap of about 0.5 eV. More recently, angle-resolved photoemission spectroscopy (ARPES) has revealed small CDW gaps that extend from 20 to 100 meV.[9] A larger gap implies strong coupling, while regions with smaller gaps seem to be characterized by imperfect nesting. Since $CeTe_2$ is essentially a quasi-2D material, the Fermi surface is partially gapped by the CDW transition. The remnant ungapped Fermi surface possesses charge carriers contributing to the electrical conductivity at low temperatures.

In this paper, we report the optical properties of $CeTe_2$ at low photon energies from the terahertz to infrared regions. Two features that correspond to large CDW gaps due to perfect nesting and small gaps due to imperfect nesting were observed at about 0.5 eV and 10 meV, respectively. In addition, a Drude response due to the collective motion of charge carriers existing on ungapped Fermi surfaces is also observed in the terahertz regions.

II. EXPERIMENT AND RESULTS

The optical reflectivity was measured on the $E\|ab$ plane and $E\|c$ axis on a single $CeTe_2$ crystal, which was grown using a slow cooling method in a sealed tungsten crucible, as described in Ref. 10. The crystal grown by this technique was stoichiometric, with the composition $CeTe_{2\pm0.02}$, which was determined by electron microprobe analysis. The cleaved ab surface and the surface perpendicular to it polished carefully in a glove box under a He-gas atmosphere were measured. Martin-Puplett and Michelson-type rapid-scan Fourier spectrometers were used at photon energy ranges from 2–30 meV and 10–1.5 eV, respectively, at sample temperatures between 7 and 300 K. To obtain the absolute reflectivity spectra, reference spectra of the sample evaporated with gold *in situ* were measured. In the energy region between 1.5 and 5 eV, the reflectivity reported in Ref. 11 was used.

Figure 1 shows the reflectivity spectra, $R(\omega)$, of $CeTe_2$ for the $E\|ab$ plane at several temperatures. The reflectivity spectra were strongly dependent on temperature over the entire spectral range. This differs from previous data reported in Ref. 8, in which $R(\omega)$ did not display any temperature dependence between 300 and 10 K. The surface of the sample used to obtain the previous data[8] was polished, and the oxidization of the surface seems to have caused the temperature independence. $R(\omega)$ approached total reflection for photon energies near zero with a minimum at about 0.4 eV, which is typical of an overall metallic behavior. Peaks due to transverse-optical (TO) phonons were observed around 0.015 eV. Optical phonons are difficult to observe in the reflectivity spectra of a metallic system because the optical phonon is well screened by free electrons. In $R(\omega)$ for CeSb, with an energy of reflectivity minimum similar to that of $CeTe_2$, the optical phonon was not observed.[12]

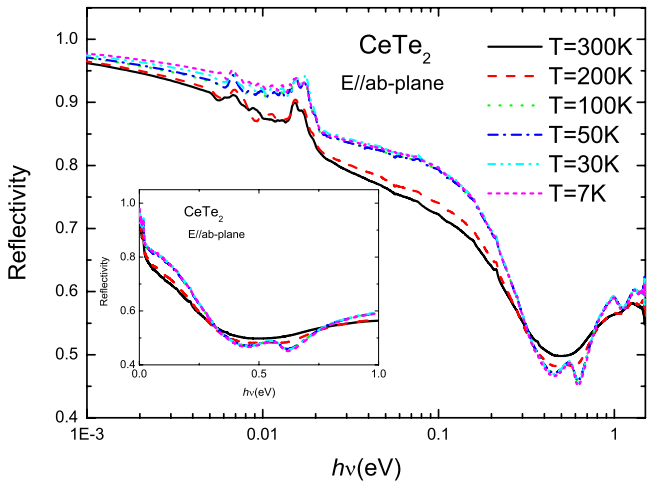

FIG. 1. (Color online) Reflectivity spectra, $R(\omega)$, of $CeTe_2$ for the $E\|ab$ plane on a logarithmic scale for temperatures in the range 7–300 K. Inset: $R(\omega)$ on a linear scale.

The inset of Fig. 1 displays $R(\omega)$ on a linear scale. At photon energy regimes lower than the reflectivity minimum, $R(\omega)$ was abnormally small compared to that of CeSb and Yb_4As_3 with low carriers.[12,13] The small reflectivity was due to the anisotropy of the CDW gaps mentioned below.

Figure 2 shows the reflectivity spectra, $R(\omega)$, for the $E\|c$ axis of $CeTe_2$ at several temperatures. The reflectivity spectra were weakly dependent on temperature over the entire spectral range. In $R(\omega)$, the metallic behavior was not seen across the entire range but an anomaly due to the TO phonon was observed around 0.018 eV. $R(\omega)$ increased slowly at photon energy regions higher than 0.3 eV. Our analysis used the optical conductivity spectra derived from the Kramers-Kronig (KK) transformation of the reflectivity spectra. For the KK transformation, we used extrapolation functions below 2 meV and above 5 eV. Below 2 meV, the extended Hagen-Rubens function, $R(\omega)=1-\sqrt{\tau_D\omega}/(1+\sqrt{\tau_D\omega}/2+\tau_D\omega/4)$, was used because the conductivity is very low. Here, τ_D is equal to $2/\pi\sigma_D$, where σ_D denotes the direct current conductivity. Above 5 eV, we used the extrapolation function, $R(\omega)=C\omega^{-4}$, where C is a fitting constant.

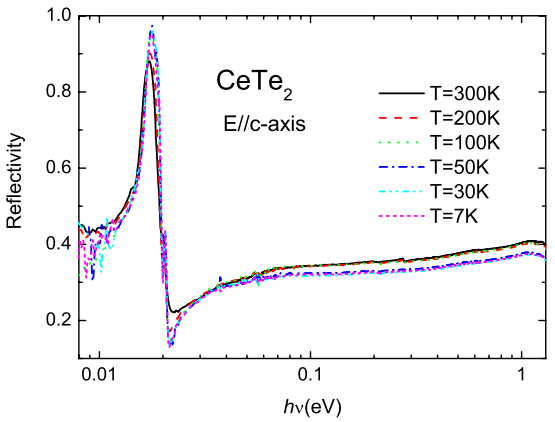

FIG. 2. (Color online) Reflectivity spectra, $R(\omega)$, of $CeTe_2$ for the $E\|c$ axis on a logarithmic scale for temperatures in the range 7–300 K.

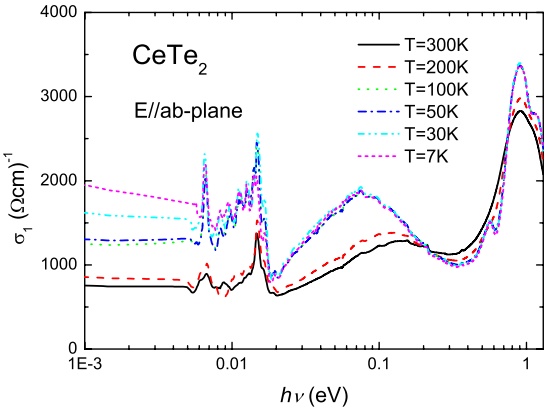

FIG. 3. (Color online) Optical conductivity spectra, $\sigma_1(\omega)$, of $CeTe_2$ for the $E\|ab$ plane on a logarithmic scale for temperatures in the range 7–300 K.

The real part of optical conductivity $\sigma_1(\omega)$ for the $E\|ab$ plane is shown in Fig. 3. The optical conductivity below 8 meV shows a metallic behavior of which it increases with decreasing temperature. Its magnitude corresponds to that of metals with low carriers. The metallic optical behavior can be understood by a Drude response. In the energy regions showing the Drude response, we also observed peaks, which are attributed to the TO phonon, around 15 meV and two midinfrared peaks around 0.57 and 0.09 eV. The peak shown at 0.57 eV was similar to that of the peak shown around 0.4 eV in previous work.[8] This peak is regarded as the excitation across a CDW gap coming from perfect nesting, but strong temperature dependence was observed in our data.

On the other hand, the peak shown at 0.09 eV changed broadly and the center of the peak shifted abruptly to a higher energy at temperatures greater than 200 K. The peak was characterized by a long tail at higher energies, and thus it cannot be considered a single excitation. When the center of the peak is positioned toward lower energies, this indicates the existence of several excitations at energies lower than that of the center energy. The peak thus arises from excitations across small CDW gaps, which are formed by imperfect nesting, and their magnitudes are various. Note that the energy of a CDW gap is dependent on a measure of the deviation from perfect nesting. In fact, small CDW gaps due to imperfect nesting are observed in ARPES for $CeTe_2$.[9] A tight-binding band-structure calculation revealed the presence of excitations due to electronic interband transitions above 1 eV.[3–5] Some peaks observed around 1 eV were due to the interband transitions seen in the band calculation.

In $\sigma_1(\omega)$ for the $E\|c$ axis shown in Fig. 4, the metallic Drude response was not observed even at the lowest photon energy, but a sharp peak was observed around 0.017 eV. The center of the peak changed linearly from 16.7 to 16.25 meV with increasing temperature. The width of the peak increased slightly. These features are known to be absorptions of TO phonons. The optical conductivity abruptly increased around 0.3 eV due to excitations across CDW gaps such as those described in the $E\|ab$ plane.

III. DISCUSSION

The optical conductivity below the spectra region showing interband transitions mainly consisted of a Drude re-

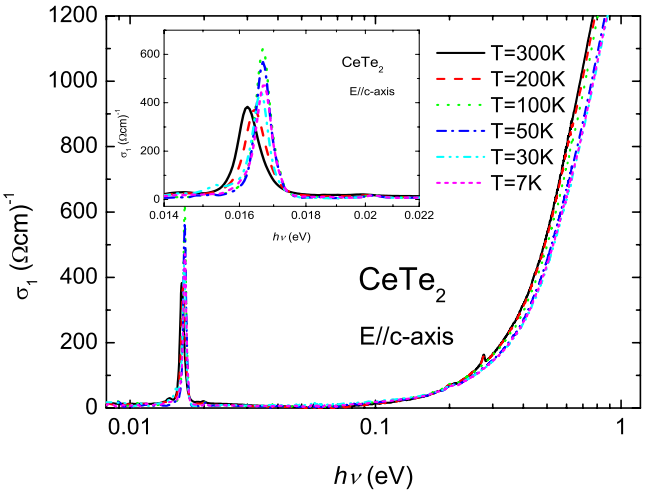

FIG. 4. (Color online) Optical conductivity spectra, $\sigma_1(\omega)$, of $CeTe_2$ for the $E\|c$ axis on a logarithmic scale for temperatures in the range 7–300 K. Inset: $\sigma_1(\omega)$ on a linear scale.

sponse, which is due to free carriers, and absorptions across CDW gaps. First, we will discuss the Drude response with a Drude model. In Fig. 3 we can find $\sigma_1(\omega)$, attributed to free carriers in the $E\|ab$ plane, to be nearly constant below about 8 meV. However, we cannot observe the Drude edge since it is screened by the peaks due to TO phonons and CDW gaps mentioned above. A large error may occur when this constant optical conductivity without the Drude edge is used in the Drude fitting because of the technical trouble in a nonlinear least-squares method, which was used in the fit of our data. To eliminate this error, we use the imaginary part of the dielectric constant (ϵ_2) in the Drude fitting. In the Lorentz-Drude phenomenological approach, the dielectric function is given by the following expression:

$$\tilde{\varepsilon} = \varepsilon_1 + \iota\varepsilon_2 = \varepsilon_\infty - \frac{\omega_P^2}{\omega^2 - \iota\omega\gamma_D} + \sum_j \frac{S_j^2}{\omega^2 - \omega_j^2 - \iota\omega\gamma_j}, \quad (1)$$

where ε_∞ is the optical dielectric constant, ω_P is the plasma frequency, γ_D is the width of the Drude peak, ω_j is the center-peak frequency, γ_j is the width, and S_j^2 is the mode strength for the jth Lorentz harmonic oscillator. The measured dielectric constant ϵ_2 increases with decreasing photon energy in low-energy regions, and we can then make a fit within a small error using the Drude components of Eq. (1).

Figure 5 is a representative fitting figure at $T=7$ K. As shown in this figure, the measured data in low photon energy regions agreed well with those calculated by the Drude model. The plasma energy was evaluated to be 0.33 ± 0.03 eV by the fitting and was nearly independent of temperature. Since the obtained plasma energy is nearly equal to the energy at a minimum of reflectivity, it seems to be reasonable. This value is half that reported by previous data.[8] The difference of plasma energy seems to come from an oxidization of the surface, which is caused by the polishing, used in Ref. 8. The presence of the plasma frequency in the CDW state is clearly related to the ungapped fraction of

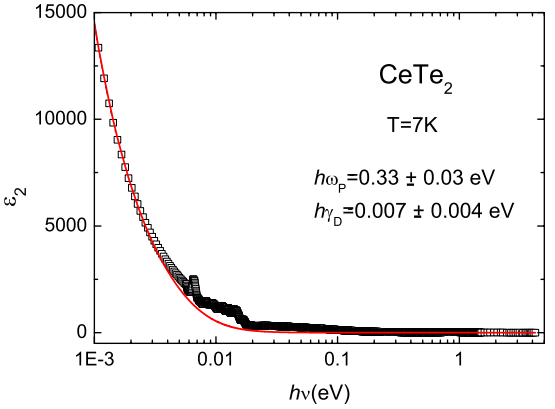

FIG. 5. (Color online) Imaginary part, ε_2, of the dielectric constant for $CeTe_2$ at $T=7$ K for $E\|ab$ plane. A solid line indicates a fitted curve by a Drude model.

the FS. The ungapped FS is also found in the ARPES of $CeTe_2$ in which free carriers contribute to the metallic behavior seen in transport measurement.

Second, we will discuss absorption across the CDW gap. To determine the size of the gap, we consider the relation between the absorption coefficient (α), which is defined as $\alpha = 2\pi\nu\epsilon_2/n$, and the photon energy ($h\nu$) given by the following equation:

$$(\alpha h\nu)^2 = A(h\nu - E_g). \quad (2)$$

Here, A, E_g, and n represent a constant, the optical band gap, and the index of refraction, respectively. E_g can be determined by extrapolations of the linear regions to zero absorption in the plots generated by Eq. (2). Figure 6 shows the relationship between $(\alpha h\nu)^2$ and $h\nu$ for $CeTe_2$ of the $E\|ab$ plane in photon energy regions, which showed a large CDW gap at $T=7$ and 300 K. The absorption coefficient remained nearly constant below 100 K. The value of α rose with increasing temperature and then flattened out to remain nearly constant at temperatures above 200 K. The large CDW en-

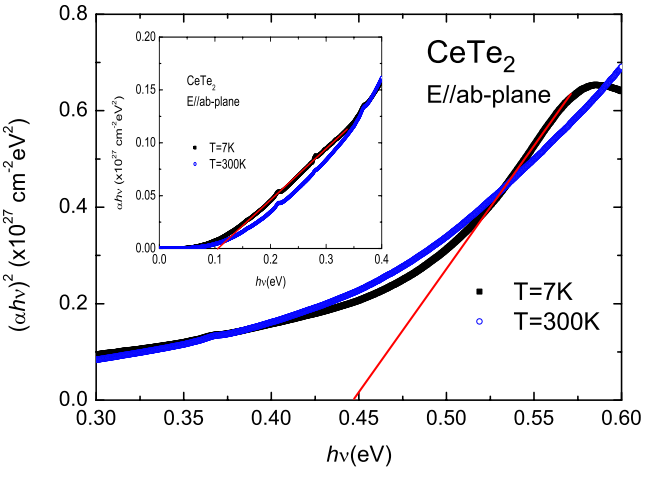

FIG. 6. (Color online) $(\alpha h\nu)^2$ vs $h\nu$ plot of $CeTe_2$ for the $E\|ab$ plane at $T=7$ and 300 K. The solid line represents a linear fit to the data. Inset: $(\alpha h\nu)^2$ vs $h\nu$ plot in lower-energy regions.

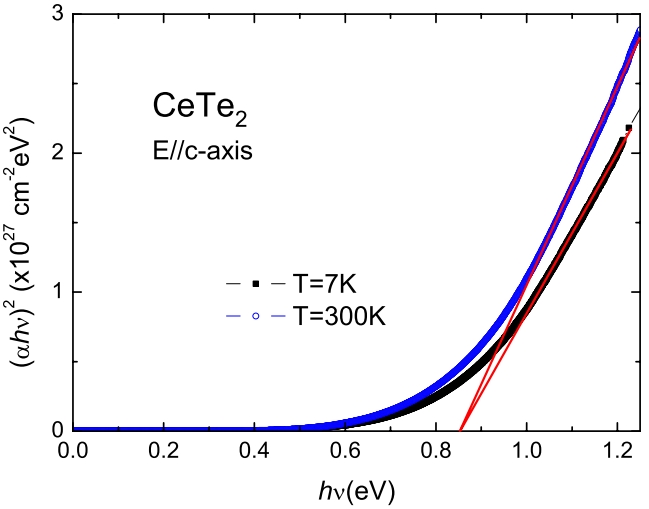

FIG. 7. (Color online) $(\alpha h\nu)^2$ vs $h\nu$ plot of $CeTe_2$ for the $E\|c$ axis at $T=7$ and 300 K. The solid line indicates a linear fit to the data.

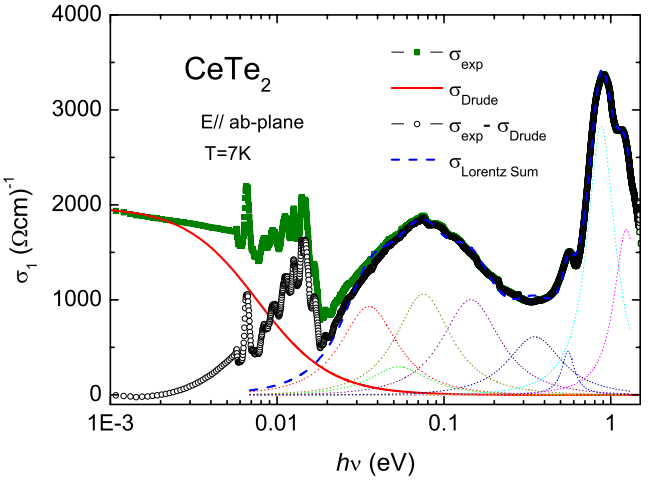

FIG. 8. (Color online) Fit of the measured optical conductivity, $\sigma_1(\omega)$, of $CeTe_2$ for the $E\|ab$ plane using the Drude and Lorentz models showing the experimental data (σ_{exp}), the total curve fitted by six Lorentz functions ($\sigma_{LorentzSum}$), and the Drude-Lorentz components (solid and dotted lines).

ergy at $T=7$ K was found to be 0.448 eV, but it was difficult to determine the size of the gap at 300 K because the linearity did not exist in the plot of $(\alpha h\nu)^2$ vs $h\nu$ due to thermal broadening.

To obtain the size of small CDW gaps we plot the relationship between $(\alpha h\nu)^2$ and $h\nu$ for lower photon energy regions in Fig. 6. As shown in the inset of Fig. 6, the linearity in the plot of $(\alpha h\nu)^2$ vs $h\nu$ is found in wide energy regions from 0.15 to 0.35 eV below 100 K and thus the small CDW energy gap at $T=7\sim100$ K was evaluated to be 109 meV, but it was difficult to determine the size of the gap above 200 K, again because of the lack of linearity. The magnitude of the large CDW gap was similar to the maximum magnitude attained by CDW gaps, which is attributed to the perfectly nesting regions of FS seen in ARPES (Ref. 3) and the tunneling experiment[1] mentioned previously in the paper. In the small CDW gap, the deviation from linearity at $T=7$ K for energies lower than 0.15 eV was, in part, due to the exciton. Small CDW gaps arising from the nonperfectly nested FS play a larger role. Recently, anisotropy of the magnitude of the CDW gap in ARPES has been found in the *ab* plane and is due to imperfect nesting. The magnitude of the gap was between 20 and 100 meV.[9] Figure 7 shows the relationship between $(\alpha h\nu)^2$ and $h\nu$ for $CeTe_2$ of the $E\|c$ axis at $T=7$ and at 300 K. The plot of this relationship is linear, and the magnitude of the CDW gap was evaluated to be 0.854 eV in all temperature regions. This value is consistent with that, 0.9 eV, obtained by tunneling measurements.[1]

The effective electron number taking part in the Drude response and the excitations across the CDW gaps is given by the formula,

$$N_{\text{eff}} = \frac{m_0}{2\pi^2 e^2 N_0}\int_0^{\omega_c} \omega\varepsilon_2(\omega)d\omega. \quad (3)$$

Here, m_0 is the rest mass of the electron, e is the electrostatic charge, and N_0 is the number of unit cells per unit volume. To evaluate the N_{eff} contributing to the Drude response shown in Fig. 8, the optical conductivity σ_{Drude}, which is calculated from parameters obtained from the Drude model fitting of ε_2, was used in the integration of Eq. (1). To evaluate the N_{eff} of the CDW peaks, we decomposed the optical conductivity by subtracting the Drude component, $\sigma_{\text{exp}}-\sigma_{\text{Drude}}$, into eight Lorentz harmonic oscillators (LHOs), as shown in Fig. 8. Among eight LHOs, six LHOs being below 0.7 eV relate to excitations between CDW gaps, whereas two LHOs above 0.7 eV relate to interband transitions. The value obtained for N_{eff} of the Drude component, $N_{\text{eff}}^{\text{Drude}}$, was 7.06×10^{-3} for $T<200$ K and increased to 7.49×10^{-3} at temperatures above 200 K. The value obtained for N_{eff} for the sum of six LHOs, $N_{\text{eff}}^{\text{Lorentz}}$, was 2.34×10^{-1} below 200 K and decreased to 2.28×10^{-1} for temperatures above 200 K. The value of $N_{\text{eff}}^{\text{Drude}}+N_{\text{eff}}^{\text{Lorentz}}$ was nearly independent of temperature. This result indicates that the gapped state at low temperatures becomes an ungapped state at higher temperatures due to thermal excitations. We propose that CDW gaps smaller than 0.1 eV exist in the *ab* plane.

The quantity $\Phi=N_{\text{eff}}^{\text{Drude}}/(N_{\text{eff}}^{\text{Drude}}+N_{\text{eff}}^{\text{Lorentz}})$ is of interest since it represents the ratio between the effective electron number of the Drude term and the total effective electron number of the Drude term and the CDW peaks. Φ roughly measures the fraction of the ungapped Fermi-surface areas that are not affected by the CDW state. Φ was estimated to be 0.029 at low temperatures and increased slightly to 0.035 at high temperatures, as explained above. The small values for Φ confirm that a large portion of the Fermi surface is gapped. Recent ARPES data provide evidence for large gapped regions on the Fermi surfaces although the ratio of the gapped region could not be determined. The presence of a very small number of carriers at the Fermi energy could be one reason for the bad metallicity observed using electrical resistivity. The value of Φ for our sample was about three times smaller than that found in previous data,[8] but the electrical resistivity was similar. This results from the fact that small CDW gaps were not found, which is thought to be due

to the broadening of energy levels caused by the oxidized surface and/or a scattering of Te vacancies, which is easy to be generated in $CeTe_2$ because of a high volatileness of Te, in the previous sample. From these data, we confirm that our sample is of good quality. Φ in our sample was similar to that seen in $CeTe_3$,[14] but $CeTe_3$ is found to possess much better metallic properties in electrical resistivity. This is not consistent with our results: $\Phi(CeTe_2) > \Phi(CeTe_3)$. This inconsistency indicates that the Fermi surface of $CeTe_3$ may be larger than that found in $CeTe_2$ or that polaronic and/or localization effects in $CeTe_2$ may play a significant role in reducing the electrical conductivity as compared to $CeTe_3$.

IV. CONCLUSION

The temperature dependence of the optical conductivity spectra of $CeTe_2$ for the $E\|ab$ plane and $E\|c$ axis were obtained in the low photon energy range 2 meV–1.5 eV. Two features of the CDW gap were observed at about 0.49 and 0.1 eV for the $E\|ab$ plane. The former corresponds to large CDW gaps due to perfect nesting, and the latter corresponds to small gaps due to imperfect nesting. We proposed that CDW gaps smaller than 0.1 eV exist in the *ab* plane, and thus the CDW gap seems to be strongly anisotropic. The gap was evaluated to be 0.854 eV on the $E\|c$ axis. In addition, a Drude response due to the collective motion of charge carriers was found in the $E\|ab$ plane. This indicates that the $CeTe_2$ is a quasi-2D material. The ratio of the ungapped Fermi surface to the gapped one was estimated to be about 3%. This value is nearly equal to that of $CeTe_3$. This indicates that the Fermi surface on $CeTe_3$ may be larger than that on $CeTe_2$ or that polaronic and/or localization effects in $CeTe_2$ may play a significant role in reducing the electrical conductivity as compared to $CeTe_3$.

ACKNOWLEDGMENTS

This work was supported by the Korea Research Foundation through Grant No. KRF-2005-070-C00044 and was performed for the Nuclear R&D Programs funded by the Ministry of Science and Technology (MOST) of Korea.

*yskwon@skku.ac.kr

[1] M. H. Jung, T. Ekino, Y. S. Kwon, and T. Takabatake, Phys. Rev. B **63**, 035101 (2000).
[2] Y. S. Kwon and B. H. Min, Physica B **281-282**, 120 (2000).
[3] K. Y. Shin, V. Brouet, N. Ru, Z. X. Shen, and I. R. Fisher, Phys. Rev. B **72**, 085132 (2005).
[4] J. Laverock, S. B. Dugdale, Zs. Major, M. A. Alam, N. Ru, I. R. Fisher, G. Santi, and E. Bruno, Phys. Rev. B **71**, 085114 (2005).
[5] A. Kikuchi, J. Phys. Soc. Jpn. **67**, 1308 (1998).
[6] B. H. Min, E. D. Moon, H. J. Im, S. O. Hong, Y. S. Kwon, D. L. Kim, and H.-C. Ri, Physica B **312-313**, 205 (2002).
[7] K. Stöwe, J. Solid State Chem. **149**, 155 (2000).
[8] M. Lavagnini, A. Sacchetti, L. Degiorgi, K. Y. Shin, and I. R. Fisher, Phys. Rev. B **75**, 205133 (2007).
[9] T. Ito (unpublished).
[10] B. H. Min, H. Y. Choi, and Y. S. Kwon, Physica B **312-313**, 203 (2002).
[11] M. H. Jung, Y. S. Kwon, T. Kinoshita, and S. Kimura, Physica B **230-232**, 151 (1997).
[12] S. Kimura, M. Okuno, H. Iwata, H. Kitazawa, G. Kido, F. Ishiyama, and O. Sakai, J. Phys. Soc. Jpn. **71**, 2200 (2002).
[13] S. Kimura, M. Okuno, H. Iwata, H. Aoki, and A. Ochiai, J. Phys. Soc. Jpn. **70**, 2829 (2001).
[14] A. Sacchetti, L. Degiorgi, T. Giamarchi, N. Ru, and I. R. Fisher, Phys. Rev. B **74**, 125115 (2006).